# Reports

## Monsoon Climate of the Early Holocene: Climate Experiment with the Earth's Orbital Parameters for 9000 Years Ago

Abstract. *Values for the precession and obliquity of the earth 9000 years ago indicate that the global average solar radiation for July 9000 years ago was 7 percent greater than at present. When the estimated solar radiation values are used in a low-resolution climate model, the model simulates an intensified continent-scale monsoon circulation. This result agrees with paleoclimatic evidence from Africa, Arabia, and India that monsoon rains were stronger between 10,000 and 5000 years ago than they are today.*

High levels of lakes across parts of Africa, Arabia, and India between 10,000 and 5000 years B.P. (before present) are striking evidence for a climate different from that of modern times. This evidence is interpreted as marking the reestablishment of monsoon rains over the Sahara and the Indian subcontinent subsequent to the weak monsoons of the period during and after the glacial maximum at 18,000 years B.P. (*1*).

The earth's orbital parameters during the early Holocene may have influenced the climate through their effect on the seasonal cycle of solar radiation. To test this possibility, I conducted a sensitivity experiment by using solar radiation values for 9000 years B.P. in a low-resolution general circulation model in place of modern values. The model is global in extent and permits simulation of the regional atmospheric circulation and surface climates. Ocean surface temperature and land albedo must be specified. There are three important elements of the experiment: (i) the model's ocean surface temperature distribution for 9000 years B.P. is assumed to be the same as at present, because the solar radiation increase for June, July, and August 9000 years B.P. is largely counteracted by a solar radiation decrease for December, January, and February; (ii) the solar radiation increase for June, July, and August 9000 years B.P. warms the model's land surface (relative to the ocean) and produces an intensified summer monsoon circulation over the African-Eurasian land mass; and (iii) the simulated results for 9000 years B.P. agree with paleoclimatic evidence.

Evidence is accumulating that variations of the earth's orbital parameters (obliquity, precession, and eccentricity) played a major role in glacial-interglacial fluctuations of the past several hundred thousand years (*2*). In previous studies time-dependent models were used to simulate the climatic response to temporal changes in the latitudinal distribution of solar radiation produced by orbital variations (*3*), but most of these studies focused on solar radiation changes at high latitudes, an emphasis that is apparent in the pioneering work of Milankovitch (*4*). Several studies suggested that the increased monsoon circulation and rains during the early Holocene were related to the solar radiation changes produced by orbital variations (*5*), and my sensitivity experiment tests this possibility quantitatively.

At 9000 years B.P. obliquity was 24.23° (the modern value is 23.45°), perihelion was 30 July (the modern value is 3 January), and eccentricity was 0.0193 (the modern value is 0.0167); these factors combine to produce solar radiation differences for July that exceed 7 percent and 25 to 35 W/m$^2$ over a broad band of latitudes (*6*) (Table 1). Differences of solar radiation for the June to August average are about 6 percent.

Table 1. Latitudinal distribution of solar radiation for July 9000 years B.P. compared to modern values.

| Latitude | Solar radiation (W/m$^2$): 9000 years B.P. | Modern | Difference | Percent change |
|---|---|---|---|---|
| 81.1°N | 522 | 486 | 36 | 7.4 |
| 69.6°N | 496 | 462 | 34 | 7.5 |
| 58.0°N | 498 | 464 | 34 | 7.3 |
| 46.4°N | 513 | 478 | 35 | 7.3 |
| 34.8°N | 516 | 481 | 35 | 7.2 |
| 23.2°N | 504 | 470 | 34 | 7.2 |
| 11.6°N | 474 | 443 | 31 | 7.2 |
| 0.0° | 429 | 400 | 29 | 7.1 |
| 11.6°S | 368 | 344 | 24 | 7.1 |
| 23.2°S | 296 | 276 | 20 | 7.1 |
| 34.8°S | 214 | 200 | 14 | 7.0 |
| 46.4°S | 130 | 121 | 9 | 6.9 |
| 58.0°S | 50 | 47 | 3 | 6.8 |
| 69.6°S | 1 | 0 | 1 | |
| 81.1°S | 0 | 0 | 0 | |

A low-resolution model of the general circulation of the global atmosphere was used for the experiment (*7*). The model incorporates atmospheric dynamics based on the equations of motion, continuity, and thermodynamics. The equations are formulated in spectral terms, and the model retains longitudinal wave numbers 1 through 10 and an 11.6° by 11.25° latitude-longitude grid for spectral-grid transforms. The model has five vertical levels and includes orographic influences of mountains (and ice sheets) as well as radiative and convective processes, condensation, and evaporation. A surface heat budget is computed over land; over ocean, the surface temperature is specified.

In contrast to the climate model experiments for glacial maximum conditions (18,000 years B.P.), where the surface boundary conditions are specified from studies of the geologic record (*8*), the boundary conditions for 9000 years B.P. are set at modern values. The use of modern boundary conditions provides a clear test of the sensitivity of the model climate to the solar radiation changes. Moreover, the modern ocean surface temperatures should be a fair approximation to the conditions 9000 years B.P.

Two lines of reasoning support this approximation for the ocean surface temperatures of 9000 years B.P. First, in the North Atlantic Ocean, where temperatures at 18,000 years B.P. are much lower than those of today (*9*), the major transition to interglacial and essentially modern conditions occurs by 9000 years B.P. (*10*); it is assumed that the major transition has also occurred elsewhere. Second, because the orbital parameters at 9000 years B.P. amplify the seasonal solar radiation cycle (compared to the present) but produce almost no change in the annual average amount (*6*), the departure of the ocean temperature at 9000 years B.P. from modern values should be small. The large heat capacity of the upper mixed layer should effectively damp the seasonal ocean temperature response to the seasonal solar radiation anomalies, and there could be no large change of annual average temperature unless there was strong covariance between the amplified seasonal radiation cycle and the seasonal cycle of albedo or mixed-layer depth.

Land albedo, ground wetness, and sea-ice extent are set at modern values.


0036-8075/81/1002-0059$01.00/0 

Table 2. Simulated surface temperature and precipitation for June to August averages and annual averages for Northern Hemisphere land, Southern Hemisphere land, and the global average of land and ocean for 9000 years B.P. compared to modern values. The difference between 9000 years B.P. and the present is denoted by Δ. The significance level (S.L.) is determined from the ratio of Δ to the model standard deviation.

| Space average | Surface temperature | | | S.L. (%) | Precipitation (cm/day) | | | S.L. (%) |
|---|---|---|---|---|---|---|---|---|
| | 9000 years B.P. (°C) | Modern (°C) | Δ (K) | | 9000 years B.P. | Modern | Δ | |
| *June to August* | | | | | | | | |
| Northern Hemisphere, land | 24.5 | 23.8 | 0.7 | 1 | 0.45 | 0.41 | 0.04 | 5 |
| Southern Hemisphere, land | 2.0 | 1.7 | 0.3 | | 0.47 | 0.45 | 0.02 | |
| Global, land and ocean | 17.7 | 17.5 | 0.2 | 5 | 0.35 | 0.35 | 0 | |
| *Annual* | | | | | | | | |
| Northern Hemisphere, land | 13.2 | 13.4 | −0.2 | | 0.39 | 0.37 | 0.02 | 5 |
| Southern Hemisphere, land | 7.5 | 7.3 | 0.2 | 5 | 0.45 | 0.47 | −0.02 | |
| Global, land and ocean | 15.9 | 15.9 | 0 | | 0.33 | 0.33 | 0 | |

At 9000 years B.P. the Scandinavian ice sheet has almost disappeared, but the North American ice sheet still extends to the northern edge of Lake Superior (*11*). The omission of the Laurentide ice sheet from the lower boundary of the model causes an unrealistic simulation of the North American climate but should not influence greatly the results over the African-Eurasian land mass that are of primary interest here. Subsequent experiments should include more realistic surface boundary conditions in order to evaluate the relative importance of solar radiation changes compared to other factors, such as the influence of ice sheets.

The starting date for the simulation of 9000 years B.P. is 1 April of year 3 of a 5-year model simulation of the modern climate (*7*). In April of 9000 years B.P. the solar radiation is close to modern values, so that the simulated modern climate changes gradually to the simulated climate for 9000 years B.P. as the seasonal solar radiation cycle proceeds from April to the increased solar radiation of May through August (*6*). The surface boundary conditions of ocean temperature and land albedo are changed, as the integration proceeds, in a smooth fashion that corresponds to the modern seasonal cycle. Certain differences between the experiment for 9000 years B.P. and the modern (control) experiment for July, for the June to August average, and for the annual average (12 months, June to June) are described. Most of these differences are well above the noise level of the model. The noise level is estimated by the standard deviations of climatic variables that are calculated from a 5-year simulation of modern climate (*7*).

The increased solar radiation of June to August 9000 years B.P. causes an increased heating of the land surface and the overlying atmosphere, a warmer land surface relative to the surrounding ocean, and a monsoon-like adjustment of the distribution of atmospheric mass. Although the increased solar radiation occurs in both hemispheres, the atmospheric response is largest north of the equator. This is because the Northern Hemisphere contains the large African-Eurasian land mass, whereas the Southern Hemisphere is largely ocean.

The surface temperature of July 9000 years B.P. is 5 K higher than in the modern simulation over north-central Asia. The difference exceeds 5 standard deviations. Between 46° and 70°N, the latitude average difference in temperature of the land surface exceeds 2 K (warmer during July 9000 years B.P.). Compared to modern conditions, the geopotential height of the near-surface pressure level (900 mbar) decreases to the north of 23°N (Fig. 1a). The largest decrease of the 900-mbar height occurs over Eurasia between 23° and 46°N and between 45° and 100°E, where the decrease exceeds 3 standard deviations. The geopotential height at the center of the 900-mbar monsoon low (located near 35°N, 90°E for the simulated climate) is decreased by 86 m (691 m for July 9000 years B.P. compared to 777 m now). This major result is reflected in the 900-mbar geopotential height differences (June to August 9000 years B.P. minus modern) averaged by latitude and partitioned by land and ocean fraction (Fig. 1b). The 900-mbar height decreases more over land than over ocean, and this altered low-level pressure distribution is associated with increased flow of air from ocean to land at low levels (that is, flow from high to low pressure).

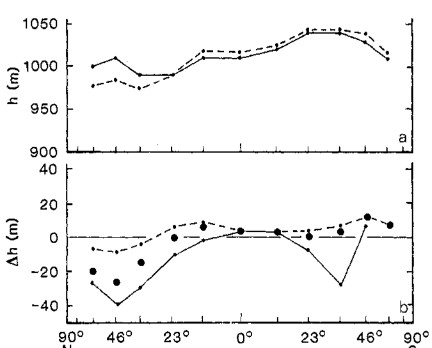


Fig. 1. (a) Simulated June to August 900-mbar latitudinal average geopotential height $h$ for 9000 years B.P. (dashed line) and the present (solid line). (b) Height differences $\Delta h$ (9000 years B.P. minus the present): (●) over land and ocean, (solid line) over land, and (dashed line) over ocean. Negative differences indicate decreased height (lower pressure) at 9000 years B.P. compared to the present. Model standard deviations (based on independent modern simulations) are typically 5 to 10 m. Height differences over land at 58°N, 46°N, and 35°N exceed 3 standard deviations. Heights and height differences are not shown for polar latitudes because the model standard deviations exceed 20 m in those regions. Heights (in meters) are graphed as a function of the sine of the latitude.

Over the African-Eurasian land mass both the low-level cyclonic inflow of air and the high-troposphere anticyclonic outflow of air are stronger at 9000 years B.P. than at present. At the surface, increased southwesterly winds carry moisture into West Africa and India. Over the Arabian Sea, the southwesterlies are 15 m/sec during July 9000 years B.P. compared to 10 m/sec for the modern simulation. The cross-equatorial flow from the Southern Hemisphere to the Northern Hemisphere over Africa and the western Indian Ocean is 4 m/sec, compared to 2 m/sec now. In the upper troposphere, the tropical easterly jet stream is more than 10 m/sec stronger during July 9000 years B.P. than in modern July over the western Indian Ocean and equatorial Africa. Along 12°N over Africa, the precipitation is about 0.6 cm/day for June to August 9000 years B.P., compared to about 0.55 cm/day now, an increase of 10 percent. Between 23° and 35°N over Arabia, India, and southeast Asia, the precipitation is about 0.75 cm/day for June to August 9000 years B.P. and about 0.5 cm/day now, an increase of 50 percent.

The precipitation rate averaged for the Northern Hemisphere land is 8 percent higher for June to August 9000 years B.P. than for the modern case; for the Southern Hemisphere land the increase is 4 percent (Table 2). This increase over the land is compensated by a decrease over the ocean, so that the global average (land plus ocean) rate for June to August 9000 years B.P. is the same as the present one. The surface temperature averaged over the Northern Hemisphere land is 0.7 K higher for June to August 9000 years B.P. The global average increase of surface temperature is only 0.2 K because the 0.7 K increase of land surface temperature is averaged with zero change for ocean surface temperature (Table 2).

The simulated intensification of the Northern Hemisphere summer monsoon agrees with paleoclimatic evidence in Africa and the Middle East of enlarged lakes during early Holocene time (*1*). Hydrological and energy balance studies of enlarged paleolakes of West Africa, East Africa, and northwest India yield estimates of precipitation increases (compared to modern values) of 20 to 100 percent (*12*). The results of this experiment for 9000 years B.P. are in fair agreement with other results based on records of lake levels, alluvial records, pollen records of more mesic vegetation types, and ocean core records of monsoon-related upwelling (*13*). The model results are also of interest for studies of the cultural history of Africa and the Near East in early Holocene time (*14*).

The period of enlarged paleolakes is restricted to 10,000 to 5000 years B.P. (*1*). This interval corresponds roughly with the interval of increased solar radiation for Northern Hemisphere summer, which peaked around 10,000 to 9000 years B.P. and returned close to modern values by 5000 years B.P. (*6*). A previous interval of high lake levels at 30,000 to 25,000 years B.P. (*1*) corresponds with a solar radiation regime that is similar to the pattern for 9000 years B.P. at tropical latitudes because of the approximate 21,000-year period of the precession cycle (*6*).

The opposite segment of the seasonal solar radiation cycle of 9000 years B.P. (December, January, and February) also influences the simulated climate. During January 9000 years B.P. the solar radiation is 7 percent less than at present over a broad latitudinal band and, in the simulation experiment, the land cools relative to the ocean. Because of compensating effects of the seasonal radiation extremes, a full annual-cycle simulation is required in order to summarize the climate's sensitivity to orbital parameter changes (Table 2) (*15*). The annual and global average values for surface temperature and pressure do not change.

Evidence for important feedback relations between ocean, atmosphere, and ice sheets on the time scale of the orbital variations (*10*) has been ignored in this experiment, as have possible land surface or $CO_2$ feedbacks (*16*). Including these factors in models, repeating the sensitivity experiment with different models, and conducting detailed validation studies (*17*) remain tasks for the future.

JOHN E. KUTZBACH
*Center for Climatic Research and Department of Meteorology, University of Wisconsin, Madison 53706*

### References and Notes

1. F. A. Street and A. T. Grove, *Quat. Res. (N.Y.)* **12**, 83 (1979); W. L. Prell *et al.*, *ibid.* **14**, 309 (1980).
2. J. D. Hays, J. Imbrie, N. J. Shackleton, *Science* **194**, 1121 (1976); J. Imbrie and J. Z. Imbrie, *ibid.* **207**, 943 (1980).
3. M. J. Suarez and I. M. Held, *Nature (London)* **263**, 46 (1976); *J. Geophys. Res.* **84**, 4825 (1979); S. H. Schneider and S. L. Thompson, *Quat. Res. (N.Y.)* **12**, 188 (1979).
4. M. Milankovitch, *K. Serb. Akad. Beogr. Spec. Publ. 132* (1941) (translated by the Israel Program for Scientific Translations, Jerusalem, 1969).
5. F. E. Zeuner, *The Pleistocene Period—Its Climate, Chronology, and Faunal Successions* (Hutchinson, London, 1959); W. L. Prell, abstract, 61st annual meeting of the American Meteorological Society, San Diego, Calif., 19 to 22 January 1981; R. A. Bryson and A. M. Swain, *Quat. Res. (N.Y.)*, in press; B. J. Mason, *Q. J. R. Meteorol. Soc.* **102**, 473 (1976). The Mason article contains a report by A. Gilchrist on a climate model experiment for May and June 10,000 years B.P. where the simulated climate was warmer than present.
6. A. L. Berger, *Quat. Res. (N.Y.)* **9**, 139 (1978); E. Hopkins, thesis, University of Wisconsin, Madison (1981). An algorithm developed by Hopkins was used to produce Table 1 and to calculate the solar radiation for the experiment. The solar radiation values in Table 1 are averages for the entire month and differ somewhat from midmonth values calculated by Berger. These solar radiation values were calculated for calendar dates relative to a vernal equinox that was fixed at 21 March. Because of the slight difference in eccentricity between 9000 years B.P. and the present, global average and annual average solar radiation was 0.005 percent higher then. Using the estimate that a 1 percent change of solar constant produces a 1.8 K change of temperature [R. T. Wetherald and S. Manabe, *J. Atmos. Sci.* **32**, 2044 (1975)], a global average temperature increase for 9000 years B.P. (relative to the present) of about 0.01 K is expected.
7. B. L. Otto-Bliesner, thesis, University of Wisconsin, Madison (1980); ———, G. W. Branstator, D. D. Houghton, *J. Atmos. Sci.*, in press.
8. W. L. Gates, *Science* **191**, 1138 (1976); *J. Atmos. Sci.* **33**, 1844 (1976); S. Manabe and D. G. Hahn, *J. Geophys. Res.* **82**, 3889 (1977); J. Williams, R. Barry, W. Washington, *J. Appl. Meteorol.* **13**, 305 (1974).
9. CLIMAP Project Members, *Science* **191**, 1131 (1976).
10. W. F. Ruddiman and A. McIntyre, *Quat. Res. (N.Y.)* **3**, 117 (1973); *Science* **212**, 617 (1981). Studies of the observational record from ocean cores will be needed to test the assumption that ocean temperatures at 9000 years B.P. were near modern values.
11. R. A. Bryson, W. M. Wendland, J. D. Ives, J. T. Andrews, *Arct. Alp. Res.* **1**, 1 (1969); H. H. Lamb, *Climate: Present, Past and Future*, vol. 2, *Climatic History and the Future* (Methuen, London, 1977).
12. J. E. Kutzbach, *Quat. Res. (N.Y.)* **14**, 210 (1980); A. Swain, J. Kutzbach, S. Hastenrath, in preparation.
13. K. W. Butzer, G. L. Isaac, J. L. Richardson, C. Washbourn-Kamau, *Science* **175**, 1069 (1972); F. A. Street, *Palaeoecol. Afr.* **11**, 135 (1979); G. Wickens, *Boissiera* **24**, 43 (1975); J. Maley, *Nature (London)* **269**, 573 (1977); G. Singh, R. D. Joshi, A. B. Singh, *Quat. Res. (N.Y.)* **2**, 496 (1972); D. A. Adamson, F. Gasse, F. A. Street, M. A. J. Williams, *Nature (London)* **287**, 50 (1980); W. L. Prell, abstract, NATO Conference on "Coastal Upwelling: Its Sediment Record," Vilamoura/Algarve, Portugal, September 1981.
14. K. W. Butzer, *Environment and Archeology: An Ecological Approach to Prehistory* (Aldine-Atherton, Chicago, 1971).
15. J. E. Kutzbach and B. L. Otto-Bliesner are preparing a complete report on this sensitivity experiment for an entire seasonal cycle.
16. S. L. Thompson and S. H. Schneider, *Nature (London)* **290**, 9 (1981).
17. G. M. Peterson, T. Webb III, J. E. Kutzbach, T. van der Hammen, T. A. Wijmstra, F. A. Street, *Quat. Res. (N.Y.)* **12**, 47 (1979).
18. Research grants ATM79-16443 and ATM79-26039 to the University of Wisconsin, Madison, from the National Science Foundation's Climate Dynamics Program supported this work. I thank B. Otto-Bliesner for collaboration in the use of the low-resolution general circulation model, P. Guetter for performing the computations, and E. Hopkins for the algorithm used to calculate the solar radiation for 9000 years B.P. The computations were made at the National Center for Atmospheric Research (NCAR), Boulder, Colo., with a computing grant from the NCAR Computing Facility.

15 May 1981; revised 27 July 1981

## Chlorine Monoxide Radical, Ozone, and Hydrogen Peroxide: Stratospheric Measurements by Microwave Limb Sounding

Abstract. *Profiles of stratospheric ozone and chlorine monoxide radical (ClO) have been obtained from balloon measurements of atmospheric limb thermal emission at millimeter wavelengths. The ClO measurements, important for assessing the predicted depletion of stratospheric ozone by chlorine from industrial sources, are in close agreement with present theory. The predicted decrease of ClO at sunset was measured. A tentative value for the stratospheric abundance of hydrogen peroxide was also determined.*

As part of NASA's Upper Atmosphere Research Program, we have developed a balloon-borne microwave limb sounder (BMLS) to perform measurements of the earth's stratosphere. The BMLS is tuned to simultaneously measure thermal emission in three spectral bands near 205 GHz (wavelength, 1.5 mm), where rotational lines of ClO, $O_3$, and $H_2O_2$ occur. This choice for initial tuning was based on the need for more measurements of ClO to help understand the catalytic depletion of stratospheric $O_3$ by chlorine from industrial sources (*1*). The nearby $H_2O_2$ band was included because stratospheric $H_2O_2$, for which no measurements have yet been reported, may be important in $O_3$ - $HO_x$ chemistry. Our first flight with the BMLS was from the National Scientific Balloon Facility in Palestine, Texas (32°N, 96°W), on 20 February 1981. This


0036-8075/81/1002-0061$01.00/0 